Yield stress measurement for earth-based building materials: the weighted plunger test

Julia Tourtelot, Imen Ghattassi, Robert Le Roy, Ann Bourgès, Emmanuel Keita

Yield stress measurement for earth-based building materials: The Weighted Plunger Test

Julia Tourtelot [1,2,3], Imen Ghattassi[4], Robert Le Roy[4], Ann Bourgès[2,3,5], Emmanuel Keita[1*]

[1] *Laboratoire Navier, Université Gustave Eiffel, ENPC, CNRS, F-77447 Marne-la-Vallée, France*

[2] *Laboratoire de Recherche des Monuments Historiques, 29 rue de Paris, 77 420 Champs-sur-Marne, France*

[3] *Sorbonne Universités, Centre de Recherche sur la Conservation (CRC, USR 3224), MNHN-MCC-CNRS, 36 rue Geoffroy-Saint-Hilaire, 75005 Paris, France*

[4] *GSA Laboratory, ENSAPM, PSL University, Paris, France*

[5] *C2RMF, Centre de Recherche et de Restauration des Musées de France, Paris, France - Institut de Recherche Chimie Paris, PSL Research University, Chimie ParisTech-CNRS, UMR8247, 11 Rue Pierre et Marie Curie, 75005 Paris, France*

Corresponding author: emmanuel.keita@univ-eiffel.fr

Abstract

Earth-based building material processing is a challenge for new constructions. Moreover, field measurements to obtain the rheological properties of fresh materials are required in building applications. However, existing field-oriented tests were designed for more flowable materials, and new protocols for stiff materials are rarely available. In this paper, a field-oriented test of yield stress **is developed** for earth-based building materials accurate enough to identify small variations for demanding applications. The squeeze test is used as the reference measurement of yield stress. For pure clays and two clay-based materials, yield stresses **could not be easily** linked to two existing tests: the Atterberg limits and the falling plunger. Finally, a weighted plunger test **was used** to measure the yield stress as accurately as the squeeze test. The development of yield stress measurements for fresh earthen materials will help implement new building techniques on the field.

Keywords: Yield stress; Rheology; Clay; Earth-based building materials; Atterberg limits

1. Introduction

Sustainability and circular economy are significant issues of contemporary construction, and raw earth techniques are promising solutions [1, 2]. Some challenges are well known for **industrialization and new processes for** earth-based building materials, such as crack induced by drying shrinkage or low mechanical strength. Moreover, field measurements to obtain the rheological properties of fresh materials are required in industrial applications.

In the laboratory environment, rheometers can be used to assess the flowability of material accurately. They are sensitive pieces of equipment that measure different rheological parameters such as the yield stress or the viscosity. Clay-based materials are mostly a plastic fluid **at low shear rate** and so the main rheological characteristic to determine is the yield stress **as a function of water content** [3]. However, the sheared sample size is limited and the maximal motor torque is usually small, thus limiting measurement of yield stress to below 1 kPa [4–6]: yield stress for earthen materials used in construction range **mostly** between a few to tens of kPa [7, 8].

For higher yield stress pastes or stiff materials, squeeze samples are commonly deployed [9–11]. Such tests are used for cement pastes [12, 13], food industry [14–16] and clay-based materials [17, 18]. Numerical and experimental studies established the link between the measured forces and yield stress. Nevertheless, this test requires precision pieces of equipment which are not robust enough for use outside the laboratory. This issue is also at the origin of the development of new rheological tests for 3D printed concrete [19–21].

Consistency and workability tests have been developed for clay-based materials, for instance, to determine the onset of landslides [22–24]. The Atterberg limits commonly indicate water contents for the plastic and liquid states [25–28]. They can be determined by **existing** tests (Casagrande apparatus, noodle technique, cone penetration) [29], but such measurements are strongly operator dependent and the relationship with rheological parameters is unclear.

Field-oriented tests commonly used in construction consist in measuring the spread and the height of concrete deposits after gravitational flow [30]. These geometrical measurements are linked to the yield stress of materials [31–33]. Mortar workability can also be evaluated with a falling plunger and a shocking table [34], but the link with yield stress is not established.

For new processes, such as extruded bricks [35], self-compacting earth [36–39], 3D printing [8, 19, 40–42] or reconstituted soils [43, 44], material requirements are challenging and they are mostly linked to flowability: pumpability, extrusion, self-standing without a frame. For these demanding applications, rheological parameters need to be accurately controlled.

However, existing field-oriented tests were designed for more flowable materials, and new protocols for stiff materials are rarely available. Thus, the development of yield stress measurements for fresh earthen materials will help the implementation of new building techniques on the field.

The main purpose of this study is to develop a field-oriented test of yield stress for earth-based building materials accurate enough to identify small variations for demanding applications. In this paper, the squeeze test is used as the reference measurement of yield stress. For pure clays and two clay-based materials, we show that yield stresses cannot be linked to two tests: the Atterberg limits and the falling plunger. Finally, a weighted plunger test measuring the yield stress as accurately as the squeeze test **is developed**.

2. Materials and methods

2.1. Materials

In this study, two raw earths and three clays were used. The first raw earth is a coating earth from the "Briqueterie deWulf" in France. It contains around 10 % of clays. The second raw earth is a natural Romainville earth from the Parisian basin. It is composed of about 53 % of clays [45].

Three pure clays were used: kaolinite from Société Kaolinière Armoricaine (SOKA company, France), illite from Argile du Velay (ARVEL company, France) and montmorillonite from Argiles du Bassin Méditéranéen (ABM company, Italy). They represent the three main groups of clays: kaolinite is tetra-octahedral (TO) repetition of alumino-silicate mineral, illite and montmorillonite are tetra-octa-tetrahedral (TOT) repetition. The clays also differ by the interlayer of clay sheets cations: any for kaolinite, potassium for illite, calcium for montmorillonite. The Atterberg limits and **the cation exchange capacity (CEC)** of these pure clays are presented in Table 1. **The CEC, in milliequivalents per 100 g of dry solid, was measured through exchange with cobaltihexamine and the liquid limit was determined by the conventional method proposed by Casagrande, the plastic limit by rolling out a thread** [46].

Type of clay	Liquid limit – water content (%)	Plastic limit – water content (%)	CEC (meq/100g)
Kaolinite	51	42	2
Illite	52	47	20
Montmorillonite	135	97	102

Table 1: Atterberg limits of the three pure clays

2.2. Mixing and samples preparation

All the mixes were prepared with a planetary mixer. The powder was first poured in the mixer bowl following by the distilled water. The mortar was first mixed for one minute at a constant speed of 67 rpm. The mixing was stopped and the walls of the mixing bowl were scrapped. Then, a second mix of 30 s was applied at a constant speed of 125 rpm. Then the mixtures **rested** for at least 48h in hermetical beakers. Before testing, mixes were homogenized for 30 seconds at 67 rpm in the planetary mixer.

The dry Romainville earth was made of large aggregates; thus its preparation was adapted. **Firstly**, the water was added to the earth and then the mixture was cured for 48 hours. Secondly, after the curing time, the mixture has been mixed for one minute at a constant speed of 67 rpm. The mixing was stopped and the walls of the mixing bowl were scrapped. Then, a second mix of 30 s was applied at a constant speed of 125 rpm.

2.3. Squeeze test

The squeeze test consists in the compression of a sample between two parallel plates. A Shimadzu AUTOGRAPH AGS-X press equipped with a 1 kN force sensor was used for the experiments. Two homemade cylindrical plates made of cement and coated with a rough resin were used as contact plates.

Before testing the materials, the mixes were stored in hermetical **containers** in order to guarantee the water content of the different mixes. Samples were laid on the lower plate of the compressive device using a cylindrical mold of the same radius (R) than the plates of 19.3 mm (see Figure 1). The initial height of the samples was around 20 mm. The top plate moved at 1 mm/s over 18 mm. The force applied was measured as a function of the distance between the plates (h).

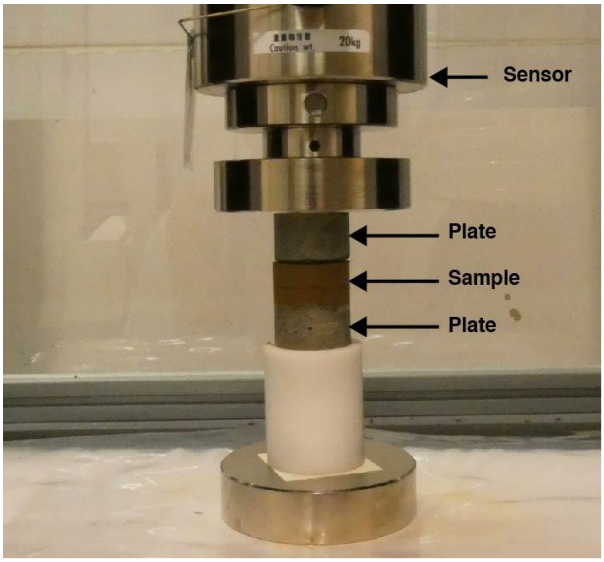

Figure 1: Squeeze test set-up

The theory of the squeeze test is well documented to calculate the yield stress [5, 9–15, 17]. Here the material does not slide at the disc surfaces and these surfaces are entirely in contact with the material at all times [9, 17]. To assess the yield stress of materials, the relationship between force and yield stress is as **follows** [10]:

$$\frac{F*h}{\pi*R^3} = \frac{2K_a}{\sqrt{3}} * \left(\frac{h}{R}\right) + \frac{2K_b}{3} \quad (1)$$

Where F is the applied force, h the spacing between the plates and R its radius. The yield stress of the slope part (K_a) corresponds to the yield stress of the bulk material. The other one (K_b) corresponds to the behavior of the material close to the plate interfaces, which is less representative. Thus, K_a **was used** to determine the yield stress of our materials.

As the squeeze test is our reference test, for comparison purposes, we may need to interpolate yield stress value. Empirically, we used an exponential fit to extend our measurements to specific water content used with the plunger tests.

2.4. Plunger test

The plunger test was carried out according to European standard NF EN 413-2:2017 (5.2 paragraph) [34]. This test is used to qualify a fresh plaster or cement-based mortar. However, it can be applied for earth-based building mortars [47].

The material fills a container (70 mm high, diameter of 80 mm). A cylinder with a hemispherical end of 25 mm diameter is connected to a graduated rod, and placed in the

center of the container. The sum of the rod and the cylinder has a weight of 90 g and is named plunger. Thus, the plunger must have a penetration distance of 35 mm after a free fall of 100 mm in a masonry mortar to meet the standard.

In this paper, the penetration distance was measured for each clay-based material at different water contents.

2.5. Weighted plunger test

The same apparatus as for the plunger test (section 2.4) was used for this modified experiment. The plunger was first placed on the surface of the **tested** material (figure 2, left: initial position) and as it was released in the paste, it enters into it without kinetic energy. Indeed, this procedure avoids viscous dissipation and focuses on yield stress.

As the standard plunger weight is fixed, it will barely indent stiff material. The penetration distance of the plunger **is measured** as its weight is increased. The plunger enters into the material under his own weight until it becomes motionless. To ensure that the equilibrium position is reached, the distance traveled by the plunger **is measured** after a 10 minutes rest. Then, the weight of the plunger was increased with successive masses placed on top of the rod (**See F**igure 2). Weights of 50, 100, 104, 200, 500 and 1000 grams were used. For each experiment, we added the masses successively until the maximum mass of 2194 grams was reached or the plunger entered over 68 mm.

Finally, the penetration height was measured as a function of the plunger weight for the five clayey materials, at least for 4 water contents for pure clays and up to 27 different water contents for the Romainville earth.

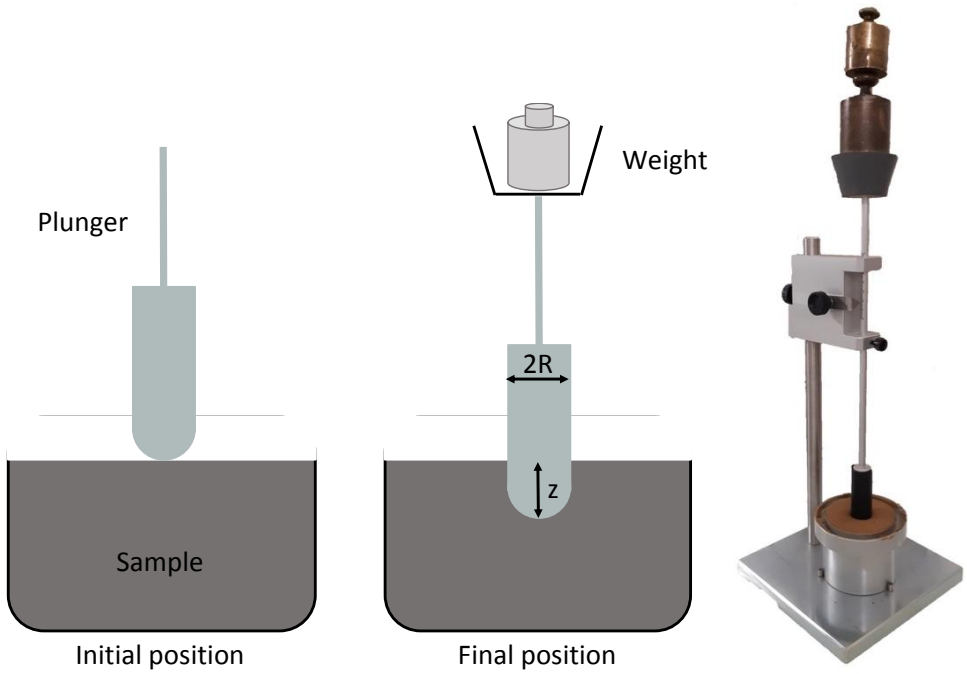

Figure 2: Scheme of the weighted plunger test. Left: initial position; Middle: final position; **Right: Picture of the set-up with a weight of m = 894 grams (see equation 2).**

3. Results

3.1. Squeeze test

In this study, the squeeze test was the reference test to assess the yield stress. Figure 3a shows a typical curve obtained during a measurement. The force was measured as a function of the height of the sample. At the beginning of the test, the plates were in contact with the material and no force was applied. As the upper plate moved, the contact between the material and the plates was completed. Then, the material was squeezed between the two plates and escaped freely by the edge; the force increases steadily (see Figure 3a). Finally, when the space between the plates has been reduced, the material was crushed and no longer flowed.

The associated stress was calculated from equation 1 (see Figure 3b). The reduced force is presented as a function of the ratio of the sample height and radius. The graph shows the placement step from h/R= 1 to 0.8 and the measurement step starting at h/R =0.8. The yield stress was then calculated from the slope formed by the curve at the measuring step.

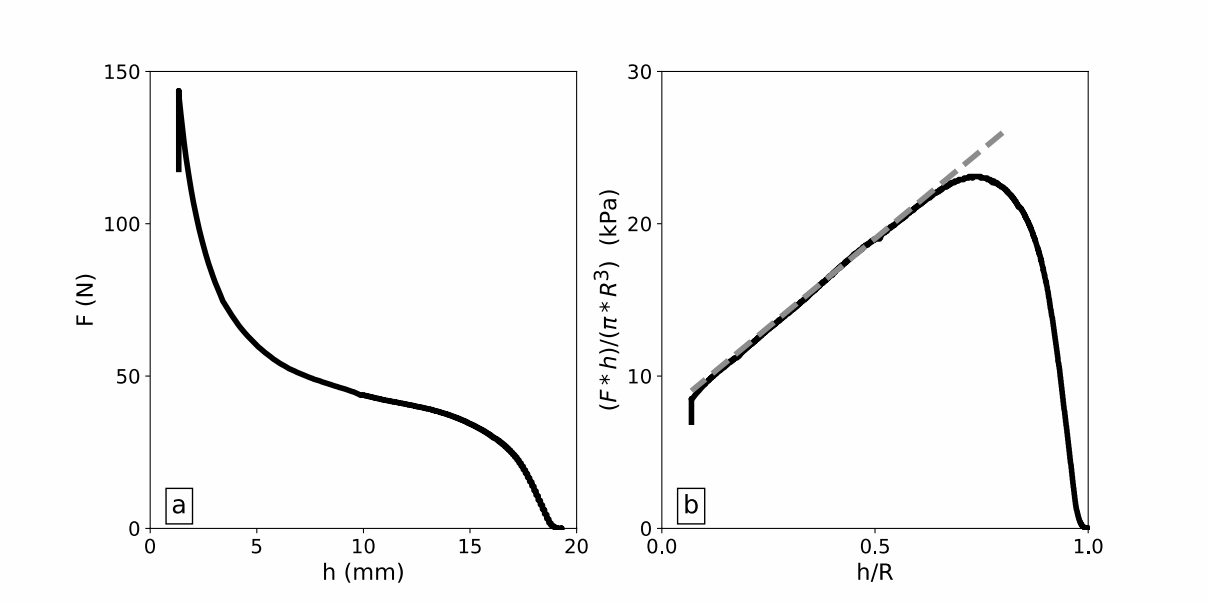

Figure 3. Montmorillonite paste **at** water content of 101 %; a: Force measured as a function of spacing between the plates (h) for squeeze test; b: Modified force, defined in equation 1, as a function of the spacing normalized by the plate radius. The dash line is the linear regression.

This gives a yield stress value for each material as a function **of** water contents (figure 4). Each clayey material has its own ranges of water content and yield stress. The highest value of yield stress is around 40 kPa and the lowest is about 0.3 kPa both for the Romainville earth. The montmorillonite shows the widest water content range from 100% to 160% while the coating earth has the narrowest from 35 to 45%. Thus, for material with a wide water content range, the variations of yield stress are easier to measure than for material with a narrow water content range.

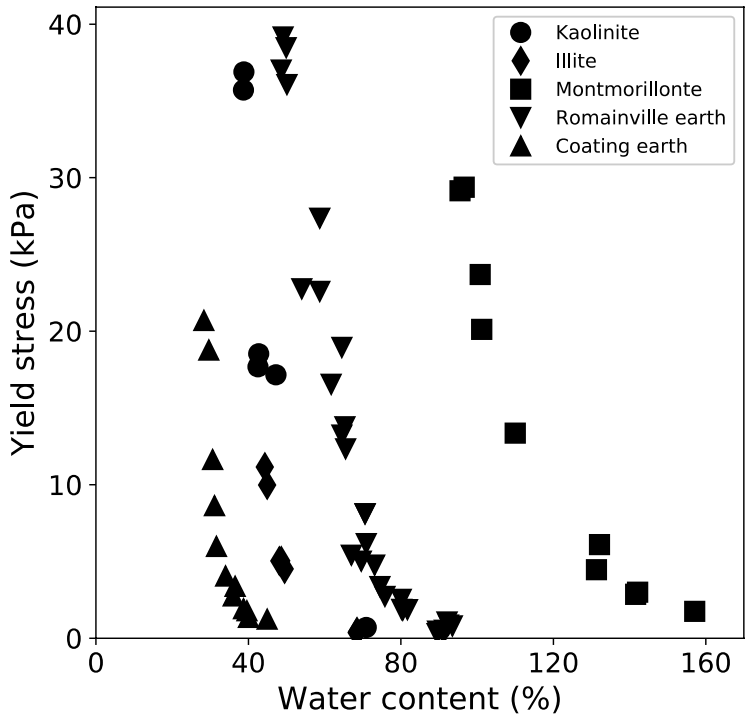

Figure 4: Yield stress measured with the squeeze test for the five clay-based materials as a function of water content

3.2. Plunger test

In a first attempt to assess the yield stress on the field, the standardized plunger test **is used**. The penetration distance of the plunger as a function of water content was measured following the standard procedure (figure 5), as described in section 2.5. This measurement was done for all the clay-based materials. We can note that the penetration distance is increasing **with** the increase of water content. The measurable range of penetration depth is between 2mm and 50 mm. For each material, it corresponds to a specific water content range. The highest depth is for illite, which reaches 47 mm at 36 % water content. The lowest depth is around 2 mm at 30 % water content for montmorillonite; this penetration depth is at the limit of our measurement. Montmorillonite has the widest range of water content measurement about 60%, while illite has the smallest range around 14%. The two clay-based materials have limited water content range around 25%. Generally, the measurable water content range is smaller than with the squeeze test.

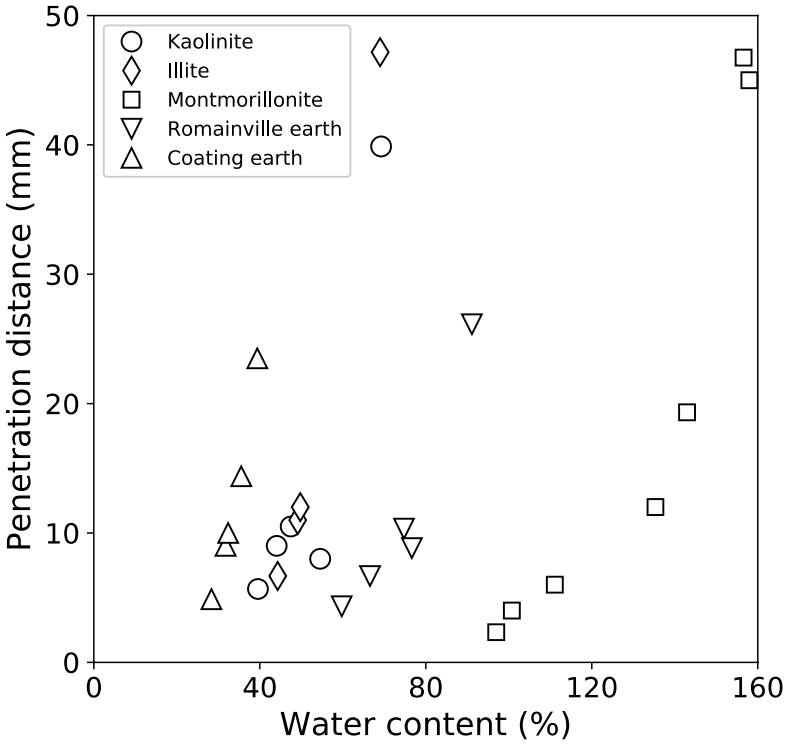

Figure 5: Penetration distance of the standard plunger as a function of water content

3.3. Weighted plunger test

To measure the yield stresses of clay-based material accurately, we adapt the plunger test by adding variable weights. Moreover, the plunger is initially at the material surface as described in section 2.5. This protocol was applied for all materials at different water contents. Figure 6 shows the increasing depth with the mass for a montmorillonite sample at 134 % water content. The penetration depth increases linearly for weight below 1kg, then the depth increases at a higher rate.

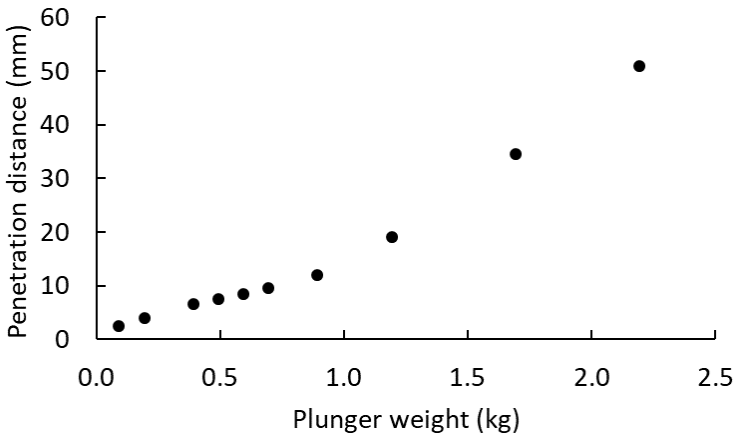

Figure 6: Distance penetration as a function of the plunger weight for the montmorillonite at a water content of 134 %

For each weight, the total forces and the yield stress are in equilibrium, so the yield stress (K_p) can be calculated with this experiment. We define the yield that is the ratio between the total forces and the surfaces at stakes [48]:

$$K_p = \frac{m*g-V_p*d_{earth}*g}{S_p} \quad (2)$$

Where m is the total mass of the weighted plunger, g the gravity acceleration, V_p the volume of the plunger immersed part, S_p its penetration surface between the plunger and material at the static equilibrium, and d_{earth} the density of the earth. The forces (numerator in equation 2) involved here are the mass of the plunger in the paste and the buoyancy in the paste against the plunger (figure 2).

In the literature, it has been shown that the geometry of the object has a strong impact on stress [48–50]. It is accepted, for example, that a horizontal object will impose greater stress than a vertical object. Several correction coefficients are proposed for the calculation of the surface at stake during the experiment depending on the object used. Note that these measurements are performed once the object is in the fluid, without calculation at the boundaries.

For the movement of a vertical plate in a fluid, a correction of (π + 2) corresponds to the coefficient of the punching stress calculation [50]. For the movement of a half-sphere in a fluid, a coefficient of 3 is proposed in accordance with Stokes' law on the displacement of a ball in a Newtonian fluid [48] or in a non-Newtonian fluid [51, 52]. As our cylinder ends with a half-sphere, the total surface is defined as the sum of the horizontal surface weighted by 3 and the vertical surface:

$$S_p = S_v + 3 * S_h \quad (3)$$

The area of the spherical cap must be considered in the calculation of S_p. Indeed, the distance traveled by the plunger is usually of the same order of magnitude as the radius of the plunger. Thus, we need to consider penetration depth as the spherical cap is partially in contact with the material, i.e. **z**< R. The surface of the spherical cap was projected horizontally and vertically. The resulting components are presented in Table 2. As z > R, this approach is compatible with the generalized surface used in [48]. Once the vertical and horizontal components of the surface have been calculated, the total surface is calculated based on equation 3.

	Horizontal surface (S_h)	*Vertical surface* (S_v)
$z < R$	$S_h = 2\pi R^2 * \left(1 - \frac{z}{2R}\right)$	$Sv = \pi R^2 * \left(\frac{\pi}{2} - \arcsin\left(1 - \frac{z}{R}\right) - \left(1 - \frac{z}{R}\right) * \frac{\sqrt{R^2 - (R-z)^2}}{R}\right)$
$z > R$	$S_h = \pi R^2$	$Sv = 2\pi R(z - R) + \frac{(\pi R)^2}{2}$

Table 2: Horizontal and vertical surfaces of the immerged plunger

Figure 7 shows a typical result obtained for a montmorillonite sample at a water content of 134 %. The total force increases **almost** linearly with the surface Sp, the change of trend around 10 N is no longer prominent. Based on equation 2, we considered the yield stress as the slope between the forces and the surface and measured it by a linear fit. In the example of Figure 7, the yield stress is about 4.5 kPa.

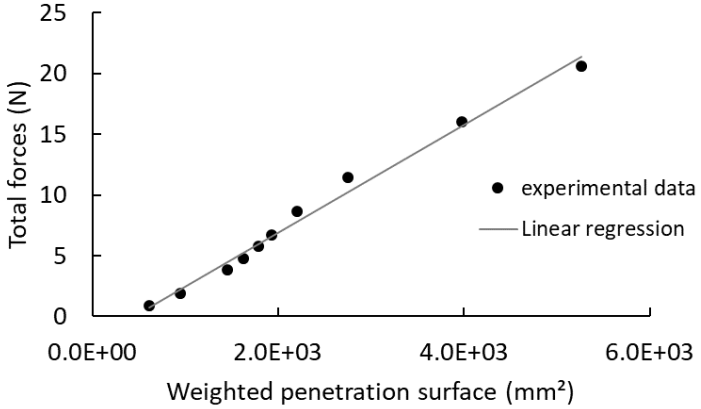

Figure 7: Total forces as a function of the weighted penetration surface for the montmorillonite at a water content of 134 %

We used this method to measure the yield stress of clay-based materials for a wide range of water contents. Figure 8 presents the yield stress measurements with the squeeze test and the weighted plunger test as a function of water content for the five materials. The points from both experiments overlap and the yield stress is decreasing with the increase of the water content. The montmorillonite has the largest range of water content to measure the yield stress, more than 60 %. On the contrary, the coating earth has a narrower range, around 20 %. **Illite and kaolinite clays have similar yield stress variations as a function of water content.**

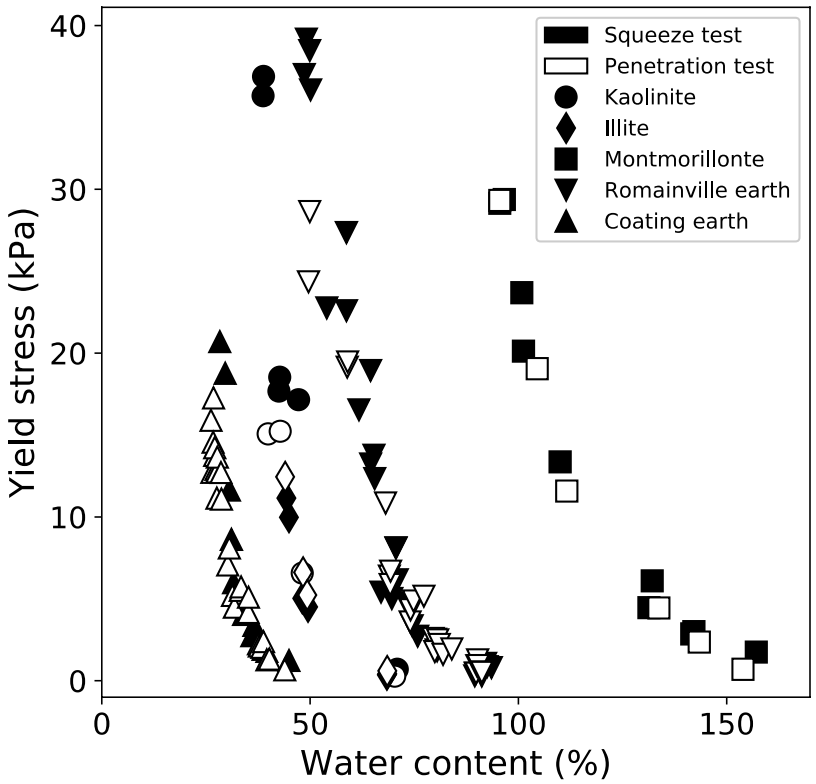

Figure 8: Yield stress measured with the squeeze test and the weighted penetration test as a function of water content

4. Discussion

The main purpose of this work is to develop a simple test to assess the yield stress of a clayey material accurate enough to identify small variations for demanding applications.

4.1. Yield stress measurements compared to Atterberg limits

The determination of Atterberg limits **by Casagrande and thread methods** is a common approach for earth-based materials [46]. We first look at the possible correlation of Atterberg limits with yield stresses as they correspond to the liquid and plastic limits of a clayey material and delimit its plastic domain.

Therefore, we plot**ted** the yield stress measured with the squeeze test as a function of the Atterberg limits for the three clays (see Figure 9). We observed that the liquid limit corresponds to a lower yield stress than the plastic limit. **However** we can see that the liquid limit has not the same value for all three clays. Illite shows the lower value while (3 kPa) and kaolinite demonstrates the greater (6.5 kPa). Similarly, the plastic limit differs strongly for the three clays. For example, the illite has the minimum value (6.7 kPa) while the montmorillonite presents the highest (28.3 kPa). Given the uncertainty, the yield stress for kaolinite at liquid limit is the same as for illite at plastic limit, around 6 kPa.

Moreover, these limits were measured on the soil fraction under 400 µm, so they are representative of the fine particles in an earthen or soil material and not on the entire fraction of the material. We know that the yield stress is a function of the distribution of the particles, so it is not the same if we consider just the fine particles or the entire fraction.

Finally, the Atterberg limits (Casagrande and thread) **could not be easily link to the yield stress, thus we suggest that they should not** be used to quantify finely the workability of earth-based building materials. **Please note that other methods to determine the Atterberg limits were correlated to yield stresses** [7, 8, 53].

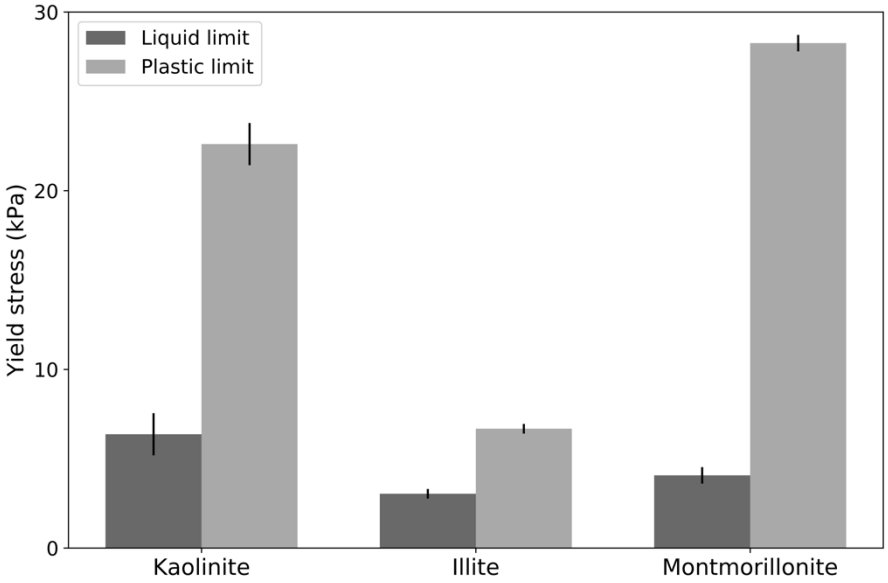

Figure 9: Yield stress measured with the squeeze test at the liquid and plastic limits for the three clays.

4.2. Yield stress compared to standard plunger test

In this section, we correlate the standard plunger test to the yield stress. Figure 10 presents the penetration height as a function of the yield stress for the five materials. All data for the different clay-based materials **seem** to **follow a similar trend**. This means that this test is not a function of the tested material and can be applied for all kinds of materials.

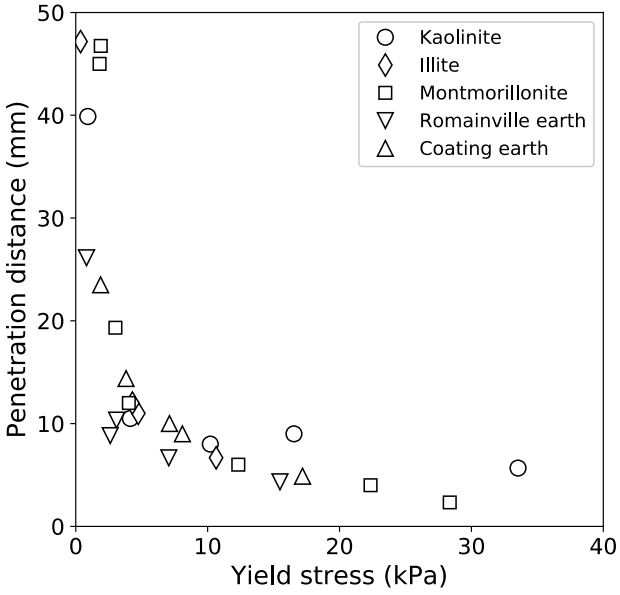

Figure 10: Penetration height during the standard falling plunger as a function of yield stress measured with the squeeze test

Nevertheless, the accurate measurement of a yield stress is difficult. Indeed the penetration has two behaviors. **First, for yield stress lower than 5 kPa, the penetration distance is above 10 mm and varies sharply. On the contrary, for yield stress above 5 kPa, the plunger barely enters the material. Therefore, this test is a great test to assess a threshold yield stress of 5kPa** [47]. However, the plunger test is not precise enough to measure the yield stress evolutions as a function of water content. Moreover, for the standard plunger, due to the free-fall over 100 mm, material viscosity may contribute to the final penetration depth. Thus the depth is not simply linked to the yield stress.

To conclude, we developed a test to improve the plunger test and measure variations in clay-based material behavior.

4.3. Squeeze test compared to weighted plunger test

To measure the yield stress with a field-oriented test, we modified the standard plunger test as described in section 2.5. The two main modifications consist in suppressing the free fall and adding various weights. Without free fall, the plunger enters slowly into the material, so that we considered the experiment as quasi-static. Moreover, to increase the range of yield stresses, the plunger should enter significantly into the stiff material. However, the initial plunger mass **was** fixed at 90 grams. Thus we choose to adapt the weight of the plunger to the material stiffness.

Figure 11 compares the results from the squeeze test and those from the weighted plunger test for the five materials tested. The dark line corresponds to **a** perfect correlation between both experiments. Thus, we can see that the experimental yield stresses from the weighted plunger test are in good agreement with those from the squeeze test.

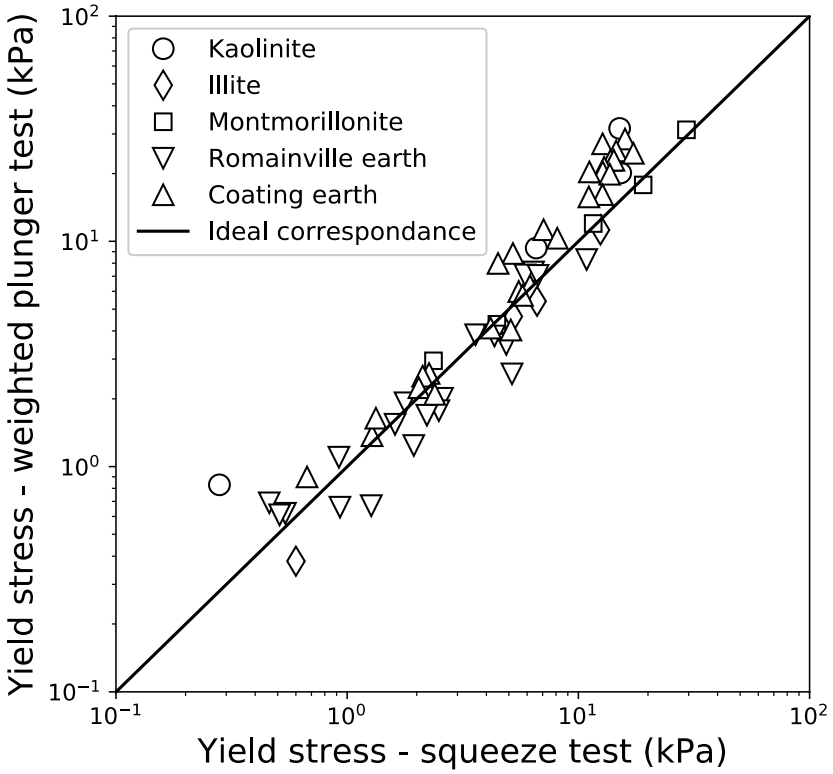

Figure 11: Comparison between the weighted penetration test and the squeeze test

To validate the correlation of the yield stresses obtained with the weighted penetration test with those of the squeeze test, six pairs of results with same water contents were compared. A statistical t-test based on Student's Law was used [54]. The mean (d = -1.38) and standard deviation (s = 3.65) of the differences in yield stress were calculated (n = six pairs of results). These values were used to calculate the experimental statistical variable t:

$$t_{exp} = \frac{d}{s/\sqrt{n}} \quad (4)$$

Its absolute value (t_{exp} = 0.93) was compared to the absolute value of the corresponding tabulated variable (t_{tab} = 2.02) at a confidence level of 90%. The inferiority of the experimental value in front of the tabulated value validated that the stress obtained with the weighted penetration test is statistically equal to the yield stress of the squeeze test. The value of t_{exp} states that the agreement between the two tests is of the same order as the standard deviation (**see Table 3**).

Material	Illite	Montmorillonite	Coating earth		Romainville earth	
Yield stress difference (kPa)	**0.18**	**0.17**	**-3.54**	**-0.51**	**-9.82**	**0.22**
Mean – d (kPa)	**-1.38**					
Standard deviation s (kPa)	**3.65**					
Pairs number – n	**6**					
t_{exp}	**-0.93**					
t_{tab}	**2.02**					

Table 3 : Statistical results of the t-test

Finally, the aim was to find out whether the two tests have the same measurement accuracy. Variances of the two tests were compared with a statistical F test based on Fischer's law [54]. For this purpose, the statistical variable F_{exp} was calculated from the ratio between the squares of the two variances. This value was compared to the statistical variable F tabulated for a confidence level of 90%. These six comparisons lead to the conclusion that for 90% of the cases, the two tests have the same accuracy.

This statistical analysis shows that, despite the simplicity of the weighted penetration test, it is possible to calculate as reliably as with the squeeze test, the yield stress of clay-based materials.

4.4. Weighted plunger test compared to existing yield stress measurements

The weighted plunger test measures yield stresses from 1 to 50 kPa with an uncertainty of 10%. In this section we compare this test to existing measurements for building materials. Rheometer measurements lays between 1Pa and 10kPa [3, 4]. Even if the range is wider, rheometers are less adapted to earth-based building materials made of large aggerates and processed directly on the field.

The field-oriented test commonly used in construction is the Abrams cone [31–33]. It is adapted for concrete with various particles size distribution. However, the yield stress range is limited from 100 Pa to 5 kPa and the uncertainty due to slippage is of the order of 20% [32]. For stiffest materials, some authors successfully increase the deformation with a free fall of the sample extending the yield stress range to 70 kPa [8]. However, this measurement **may depend on the experimenter** in the field.

Recently, measurements directly after extrusion seem promising for Concrete 3D printing [20, 21]. They are developed for concrete materials and may be applied for earth-based building materials.

4.5. Practical implementations for the weighted plunger test

The yield stress of clay materials can be measured with a penetration test providing results as accurate **as** the squeeze test. The squeeze test corresponds to a laboratory characterization test while the weighted plunger test makes it possible to measure yield stress easily with little equipment on site. We can propose some recommendations for efficient use.

With the equipment used in this study, yield stresses range from 0.2 kPa to 37 kPa. For these extreme values, we use a least three different masses to fit the experimental curve as in Figure 7, and a maximum distance traveled of 50 mm. The first condition is necessary to perform linear regression. The second condition is linked to our container height.

Indeed, these measurement limits can be extended by changing the geometries or the masses. The most straightforward parameter to vary is the force applied by changing the masses. Thus, for yield stress value lower than 0.2kPa, it will require weights of a few tens of grams, whereas for yield stress value higher than 30 kPa, it will require kilograms.

Another leverage is the radius of the plunger. For fluid material**s**, the radius of the plunger should be enlarged to increase the penetration surface and limit the distance traveled by the plunger. For stiff materials, the radius of the plunger should be decreased to facilitate its entry into the material. We need to keep in mind that it should be higher than the maximum granular diameter to maintain a homogeneous approach. In this study, the radius has been at least 10 times greater than the maximum granular diameter.

Adapting the weights and the geometry, the weighted plunger is a versatile test to measure a large range of clay-based material yield stresses accurately.

5. Conclusions

The main purpose of this study was to develop a field-oriented test to assess the yield stress for earth-based building materials accurate enough to identify small variations for demanding applications. To develop this kind of test, we used a representative selection of pure clays and two different earths. As squeeze test is a well-established method, we used it as a reference for yield stress measurements. **Firstly**, we compared Atterberg limits with the yield stress

obtained with the squeeze test and showed that the yield stress **could not be easily** linked to the Atterberg limits determined **by Casagrande and thread methods**. Then, we **showed** that the yield stress **could not be easily determined over a large range by** the standard falling plunger for our clay-based materials.

Then, we develop**ed** a weighted plunger test based on the same apparatus than for the standard plunger test. We suppressed the free fall to avoid viscous dissipation and focus on the yield stress. The principle of the test **was** to gradually increase the weight of the plunger and to measure its penetration distance into the material in order to calculate the yield stress of the material from the force and the contact surface. Base**d** on statistical analysis, we **showed** that the weighted plunger test measures the yield stress as accurately as the squeeze test. We then discussed the limits of use and the possibilities of modifications to increase the range of measurement.

In conclusion, we developed a yield stress test for earth-based building materials simple enough to be used on the field. This kind of test will be necessary for the standardization, industrialization **and usage of local materials** in the field of earthen constructions. It may also be useful for new techniques. Indeed, interest is growing for new mix-designs of earthen materials for 3D printing and extrusion that need accurate control of flowability.

Acknowledgments

This work has been carried out within the frame of the project Alluvium. Initiated in 2018, Alluvium is part of I-SITE FUTURE, a French initiative to answer the challenges of sustainable city.

We acknowledge the help of Loren Masson for the Atterberg limits measurements and Patrick Belin for his help on the implementation of the squeeze test. The authors thank Nicolas Roussel for enlightening discussions and Richard Buswell for useful comments.

Compliance with Ethical Standards

Funding: This study was funded by I-SITE FUTURE from the French Research Agency (project name: Alluvium).

References

1. Van Damme H, Houben H (2018) Earth concrete. Stabilization revisited. Cem Concr Res 114:90–102. https://doi.org/10.1016/j.cemconres.2017.02.035
2. Melià P, Ruggieri G, Sabbadini S, Dotelli G (2014) Environmental impacts of natural and conventional building materials: a case study on earth plasters. J Clean Prod 80:179–186. https://doi.org/10.1016/j.jclepro.2014.05.073
3. Ghezzehei TA, Or D (2001) Rheological Properties of Wet Soils and Clays under Steady and Oscillatory Stresses. Soil Sci Soc Am J 65:624–637. https://doi.org/10.2136/sssaj2001.653624x
4. Estellé P, Lanos C, Ea L, et al (2011) High Torque Vane Rheometer for Concrete : Principle and Validation from Rheological Measurements. 22:1–7. https://doi.org/10.3933/ApplRheol-22-12881
5. Coussot P (2005) Rheometry of Pastes, Suspensions, and Granular Materials: Applications in Industry and Environment. John Wiley & Sons
6. De Larrard F, Ferraris CF, Sedran T (1996) Fresh concrete: A Herschel-Bulkley material. Mater Struct Constr 31:494–498. https://doi.org/10.1007/bf02480474
7. Perrot A, Rangeard D, Levigneur A (2016) Linking rheological and geotechnical properties of kaolinite materials for earthen construction. Mater Struct Constr 49:4647–4655. https://doi.org/10.1617/s11527-016-0813-9
8. Perrot A, Rangeard D, Lecompte T (2018) Field-oriented tests to evaluate the workability of cob and adobe. Mater Struct Constr 51:1–10. https://doi.org/10.1617/s11527-018-1181-4
9. Engmann J, Servais C, Burbidge AS (2005) Squeeze flow theory and applications to rheometry: A review. J Nonnewton Fluid Mech 132:1–27. https://doi.org/10.1016/J.JNNFM.2005.08.007
10. Toutou Z, Roussel N, Lanos C (2005) The squeezing test: A tool to identify firm cement-based material's rheological behaviour and evaluate their extrusion ability. Cem Concr Res 35:1891–1899. https://doi.org/10.1016/j.cemconres.2004.09.007
11. Meeten GH (2004) Effects of plate roughness in squeeze-flow rheometry. J Nonnewton Fluid Mech 124:51–60. https://doi.org/10.1016/j.jnnfm.2004.07.003
12. Cardoso FA, John VM, Pileggi RG (2009) Rheological behavior of mortars under different squeezing rates. Cem Concr Res 39:748–753. https://doi.org/10.1016/j.cemconres.2009.05.014
13. Cardoso FA, John VM, Pileggi RG, Banfill PFG (2014) Characterisation of rendering mortars by squeeze-flow and rotational rheometry. Cem Concr Res 57:79–87. https://doi.org/10.1016/j.cemconres.2013.12.009
14. Huang TA (2008) Utility of squeeze flow in the food industry. AIP Conf Proc 1027:1280–1282. https://doi.org/10.1063/1.2964544
15. Estellé P, Lanos C, Mélinge Y, Servais C (2006) On the optimisation of a texture analyser in squeeze flow geometry. Meas J Int Meas Confed 39:771–777. https://doi.org/10.1016/j.measurement.2006.02.004
16. Wang YC, Muthukumarappan K, Ak MM, Gunasekaran S (1998) A device for evaluating melt/flow

characteristics of cheeses. J Texture Stud 29:43–55. https://doi.org/10.1111/j.1745-4603.1998.tb00152.x
17. Roussel N, Lanos C (2003) Plastic Fluid Flow Parameters Identification Using a Simple Squeezing Test. Appl Rheol 13:132–141. https://doi.org/10.1515/arh-2003-0009
18. Roussel N, Lanos C (2004) Particle Fluid Separation in Shear Flow of Dense Suspensions: Experimental Measurements on Squeezed Clay Pastes. Appl Rheol 141410:256–26556. https://doi.org/10.1515/arh-2004-0015
19. Perrot A, Rangeard D, Courteille E (2018) 3D printing of earth-based materials: Processing aspects. Constr Build Mater 172:670–676. https://doi.org/10.1016/j.conbuildmat.2018.04.017
20. C YJ, Picandet V, Rangeard D (2020) Gravity Driven Tests to Assess Mechanical Properties of Printable Cement-Based Materials at Fresh State. Second RILEM Int Conf Concr Digit Fabr – Digit Concr 2020 280–289. https://doi.org/10.1007/978-3-030-49916-7_29
21. Ducoulombier N, Carneau P, Mesnil R, et al (2020) " The Slug Test ": Inline Assessment of Yield Stress for Extrusion-Based Additive Manufacturing. Second RILEM Int Conf Concr Digit Fabr – Digit Concr 2020 216–224. https://doi.org/10.1007/978-3-030-49916-7_22
22. Carrière SR, Jongmans D, Chambon G, et al (2018) Rheological properties of clayey soils originating from flow-like landslides. Landslides 15:1615–1630. https://doi.org/10.1007/s10346-018-0972-6
23. Khaldoun A, Moller P, Fall A, et al (2009) Quick Clay and Landslides of Clayey Soils. Phys Rev Lett 103:1–4. https://doi.org/10.1103/PhysRevLett.103.188301
24. Coussot P, Meunier M (1996) Recognition, classification and mechanical description of debris flows. Earth-Science Rev 40:209–227. https://doi.org/10.1016/0012-8252(95)00065-8
25. NF EN ISO 17892-12:2018 Reconnaissance et essais géotechniques — Essais de laboratoire sur les sols — Partie 12 : Détermination des limites de liquidité et de plasticité
26. Fitton T, Seddon K (2012) Relating Atterberg limits to rheology. In: Proceedings of the 15th International Seminar on Paste and Thickened Tailings. pp 273–284
27. Gutiérrez A (2006) Determination of Atterberg Limits: Uncertainty and Implications. J Geotech Geoenvironmental Eng 132:420–424. https://doi.org/10.1061/(ASCE)1090-0241(2006)132:3(420)
28. Day JH, Everett KR (1972) Classification of Organic Soils. Arct Alp Res 4:283. https://doi.org/10.2307/1550232
29. Andrade FA, Al-Qureshi HA, Hotza D (2011) Measuring the plasticity of clays: A review. Appl Clay Sci 51:1–7. https://doi.org/10.1016/j.clay.2010.10.028
30. Roussel N (2007) The LCPC BOX: A cheap and simple technique for yield stress measurements of SCC. Mater Struct Constr 40:889–896. https://doi.org/10.1617/s11527-007-9230-4
31. Roussel N, Stefani C, Leroy R (2005) From mini-cone test to Abrams cone test: Measurement of cement-based materials yield stress using slump tests. Cem Concr Res 35:817–822. https://doi.org/10.1016/j.cemconres.2004.07.032
32. Roussel N, Coussot P (2005) “Fifty-cent rheometer” for yield stress measurements: From slump to spreading flow. J Rheol (N Y N Y) 49:705–718. https://doi.org/10.1122/1.1879041
33. Tan Z, Bernal SA, Provis JL (2017) Reproducible mini-slump test procedure for measuring the yield stress of cementitious pastes. Mater Struct 50:1–12. https://doi.org/10.1617/s11527-017-1103-x
34. NF EN 413-2:2017 Ciment à maçonner - Partie 2 : Méthodes d’essai

35. Khelifi H, Perrot A, Lecompte T, Ausias G (2013) Design of clay/cement mixtures for extruded building products. Mater Struct Constr 46:999–1010. https://doi.org/10.1617/s11527-012-9949-4
36. Landrou G, Brumaud C, Winnefeld F, et al (2016) Lime as an anti-plasticizer for self-compacting clay concrete. Materials (Basel) 9:. https://doi.org/10.3390/ma9050330
37. Landrou G, Brumaud C, Plötze ML, et al (2018) A fresh look at dense clay paste: Deflocculation and thixotropy mechanisms. Colloids Surfaces A Physicochem Eng Asp 539:252–260. https://doi.org/10.1016/j.colsurfa.2017.12.029
38. Achenza M, Fenu L (2007) On Earth Stabilization with Natural Polymers for Earth Masonry Construction. Mater Struct 39:21–27. https://doi.org/10.1617/s11527-005-9000-0
39. Hamard E, Cammas C, Lemercier B, et al (2019) Micromorphological description of vernacular cob process and comparison with rammed earth. Front Archit Res. https://doi.org/10.1016/j.foar.2019.06.007
40. Dubor A, Cabay E, Chronis A (2018) Energy Efficient Design for 3D Printed Earth Architecture. In: De Rycke K, Gengnagel C, Baverel O, et al (eds) Humanizing Digital Reality: Design Modelling Symposium Paris 2017. Springer Singapore, Singapore, pp 383–393
41. Ibrahim A (2019) 3D Printing Clay Facade walls | Integrating Ventilation systems into printing process. Delft University of Technology
42. Rael R, Fratello VS (2017) Clay bodies: Crafting the future with 3D printing. Archit Des 87:92–97. https://doi.org/10.1002/ad.2243
43. Ma C, Zhao B, Long G, et al (2018) Quantitative study on strength development of earth-based construction prepared by organic clay and high-efficiency soil stabilizer. Constr Build Mater 174:520–528. https://doi.org/10.1016/j.conbuildmat.2018.04.119
44. Tiwari B, Ajmera B (2011) A new correlation relating the shear strength of reconstituted soil to the proportions of clay minerals and plasticity characteristics. Appl Clay Sci 53:48–57. https://doi.org/10.1016/j.clay.2011.04.021
45. Luzu B, Duc M, Djerbi A, Gautron L (2020) High Performance Illitic Clay-Based Geopolymer: Influence of the Mechanochemical Activation Duration on the Strength Development. Calcined Clays Sustain Concr 363–373. https://doi.org/10.1007/978-981-15-2806-4_43
46. ISO 17892-12:2018 - Geotechnical investigation and testing — Laboratory testing of soil — Part 12: Determination of liquid and plastic limits
47. Bourgès A, Vergès-Belmin V (2011) Application of fresh mortar tests to poultices used for the desalination of historical masonry. Mater Struct Constr 44:1233–1240. https://doi.org/10.1617/s11527-010-9695-4
48. Lootens D, Jousset P, Martinie L, et al (2009) Yield stress during setting of cement pastes from penetration tests. Cem Concr Res 39:401–408. https://doi.org/10.1016/j.cemconres.2009.01.012
49. Uhlherr PHT, Guo J, Fang T, Tiu C (2002) Static measurement of yield stress using a cylindrical penetrometer. Korea-Australia Rhology J 14:17–23
50. Boujlel J, Coussot P (2012) Measuring yield stress: A new, practical, and precise technique derived from detailed penetrometry analysis. Rheol Acta 51:867–882. https://doi.org/10.1007/s00397-012-0643-9
51. Beris AN, Tsamopoulos JA, Armstrong RC, Brown RA (1985) Creeping motion of a sphere through a Bingham plastic. J Fluid Mech 158:219–244. https://doi.org/10.1017/S0022112085002622

52. Mitsoulis E (1998) Effect of rheological properties on the drag coefficient for creeping motion around a sphere falling in a tightly-fitting tube. J Nonnewton Fluid Mech 74:263–283. https://doi.org/10.1016/S0377-0257(97)00059-1
53. Vinceslas T (2019) Caractérisation d'éco-matériaux terre-chanvre en prenant en compte la variabilité des ressources disponibles localement. Université Bretagne Sud
54. Dekking FM, Kraaikamp C, Lopuhaä HP, Meester LE (2005) A Modern Introduction to Probability and Statistics. Springer London, London